Available online at www.banglajol.info

Bangladesh J. Sci. Ind. Res. **49(2)**, 111-118, 2014

BCSIR

BANGLADESH JOURNAL OF SCIENTIFIC AND INDUSTRIAL RESEARCH

E-mail: bjsir07@gmail.com

Adsorption of remazol red RR onto chitosan from aqueous solution

Md. Pabel Kabir[1], Md. Manuarul Islam[2], Shah Md. Masum[3], Md. Mufazzal Hossain[1*]

[1]*Department of Chemistry, University of Dhaka, Dhaka 1000, Bangladesh*
[2]*Bangladesh Council of Scientific and Industrial Research, Dhaka 1205*
[3]*Department Applied Chemistry and Chemical Engineering, University of Dhaka, Dhaka 1000*

Abstract

Chitosan has been used as an adsorbent to remove remazol red RR from aqueous solution by adsorption. The experiments have been conducted to study the effects of initial concentration of adsorbate, temperature, pH and particle size on dye adsorption. The kinetic data obtained have been examined using pseudo first- and pseudo second-order equations. The equilibrium adsorption data have been studied by using Freundlich and Langmuir models. The best results have been achieved with the pseudo second-order kinetic model and with the Langmuir equilibrium isotherm model. The equilibrium adsorption capacity (q_e) of chitosan increases with increasing the initial concentration of dye, temperature and with decreasing particle size. However, the highest adsorption capacity has been found at a pH about 5.4. The maximum monolayer adsorption capacity, q_e = 155.72 mg/g has been found at the optimum conditions. The activation energy (E_a) of sorption kinetics is about 9.25 kJ/mol. Thermodynamic parameters such as change in free energy (ΔG), enthalpy (ΔH) and entropy (ΔS) have also been evaluated.

Keywords: Chitosan; remazol red RR; Adsorption isotherms; Freundlich and Langmuir models; Kinetics of adsorption

Introduction

With economic and technological development, water pollution is becoming more and more serious problem. Dyes mainly from dyeing industries have become serious threats to human beings and the aquatic ecosystem, due to their toxicity and persistence after being released into the natural water (Tsuboy et al, 2007; Vinitnantharat et al., 2008). Therefore, discharge regulations are progressively becoming more stringent. Many recent studies have been focused on the development of efficient processes for the recovery of these organic contaminants from the effluents of textile industries (Raïs et al. 2002; Rezaee et al. 2008; Racyte et al. 1999). Usually conventional techniques such as precipitation, coagulation and flocculation have been used in wastewater treatment although these techniques are not very efficient for removing several common dyes, especially from dilute solutions (Raïs et al. 2002). Photo-oxidation has also been proposed for the treatment of dye-containing effluents (Rezaee et al. 2008; Racyte et al. 1999). However, this process is relatively expensive and not appropriate for the treatment of large flows. More recently, biological degradation has been cited as an alternative process for the decolorization of the reactive dye (Saraswathi and M. K. Saseetharan, 2010). On the other hand, adsorption processes remain the most common useful techniques for the decontamination of the effluents of textile and dyeing industries. Many studies have been made on the possibility of using different adsorbents such as mineral sorbents (Varlikli et al. 2009), activated carbons (Rodriguez et al. 2009), peat (Fernandes et al. 2007), chitin (McKay et al. 1982), rice husk (Chowdhury et al. 2009), soy meal hull (Arami et al. 2006) and agro wastes (Aksu et al. 2001). However, the adsorption capacity of the adsorbents is not very effective to improve adsorption performance and therefore, new adsorbents are still under development.

It is well known that chitosan (Fig. 1a) has widely been used in the preparation of various biomedical products (Saha et al. 2006). Chitosan is easily prepared from chitin by deacetylating its acetoamide groups with a strong alkaline solution. This is the most abundant biopolymer in nature after cellulose. The high proportions of amino functions in chitosan have been found to provide novel adsorption properties for many metal ions (Chu 2002; Rangel-Mendez et al. 2009) and organic dyes (Modak et al. 2009; Lazaridis et al. 2007; Chiou and Li 2002). The deacetylated amino groups in chitosan can be protonated and the polycationic properties of the polymer are expected to contribute to the charged

---

*Corresponding Author: E-mail: mufazzal@du.ac.bd

interactions with a model dye, remazol red RR (RRR), which is an anionic azo dye (Fig. 1b). In this study, a series of batch adsorption experiments have been carried out. The main objective of the present research is to use chitosan as an adsorbent for removal of RRR from aqueous solution and study its effectiveness as an adsorbent and evaluate the kinetic and thermodynamic parameters of adsorption.

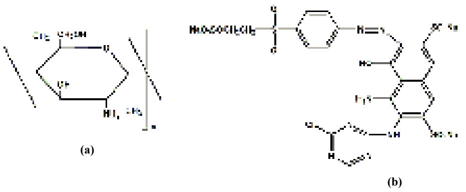

Fig. 1. Structures of (a) chitosan and (b) remazol red RR (RRR)

Experimental

Materials

Commercial grade RRR was obtained from Dyestar, Germany. All other commercial chemicals such as NaOH, $CaCl_2$ were of analar grade and were purchased from Fluka, Switzerland. Double distilled water was used throughout the present study.

The material chitosan was prepared from shrimp shell in the laboratory of Bangladesh Council of Scientific and Industrial Research (BCSIR) and used here without further purification. Indigenous shrimp shells were collected from Bagherhat, Khulna. Shrimp shells were scraped free of loose tissue, washed with cold water and dried in sun for 2 days. The shells were ground to powder by grinder. The finely powdered shrimp shells were demineralized with HCl. At room temperature, the shrimp shells were treated with 5% HCl for 24 hours with a solid to solvent ratio of 1:6(w/v). After 24 hours, the shells were quite squashy and were rinsed with distilled water to remove acid and calcium chloride and dried in an oven to 70°C. For deproteinization, the demineralized shells were treated with 6% NaOH solution for 48 hours at 60-70° C at a solid (shells) to solvent (aq. NaOH) ratio of 1:10 (w/v). The residue was collected washed with distilled water and sun dried. Finally, the material was divided into different fractions depending on their particle size using different sieves.

Batch adsorption experiments

Batch adsorption experiments were performed by varying the following parameters like initial concentration of adsorbate, temperature, pH and particle size of adsorbent. Batch adsorption experiments were carried out using different composition feed mixtures taken in various reagent bottles placed in a shaking thermostat (120 rpm). At the end of predetermined intervals, the adsorbent was separated from the centrifugate by centrifugation and the progress of adsorption was monitored spectrophotometrically using UV-1650 PC (Shimadzu, Japan) at the λ_{max} = 521 nm of the absorption spectrum of RRR. A standard calibration curve was constructed (Fig. 2) and the molar extinction coefficient was evaluated at the λ_{max}, which was 1.63×10^4 L $mol^{-1}cm^{-1}$.

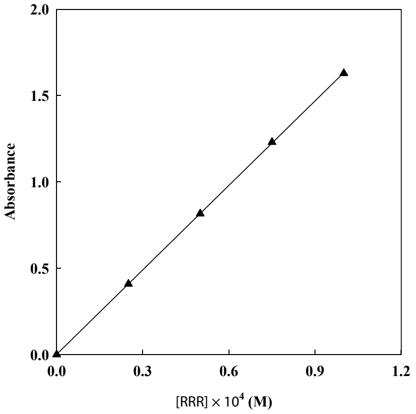

Fig. 2. Calibration curve for determination of concentration of RRR at λmax = 521 nm.

Results and Discussion

Effect of initial dye concentration

Fig. 3. shows that the effect of initial RRR concentration on the adsorption kinetics of the chitosan at pH 5.4 and temperature 30 ^{0}C. An increase in the initial dye concentration leads to an increase in the adsorption capacity of the dye on chitosan. This is due to the increase in the driving force of the concentration gradient, as an increase in the initial dye concentration (Chiou and Li 2002). Fig. 3 also shows that most of the dye is adsorbed to achieve equilibrium adsorption within 65 minutes.

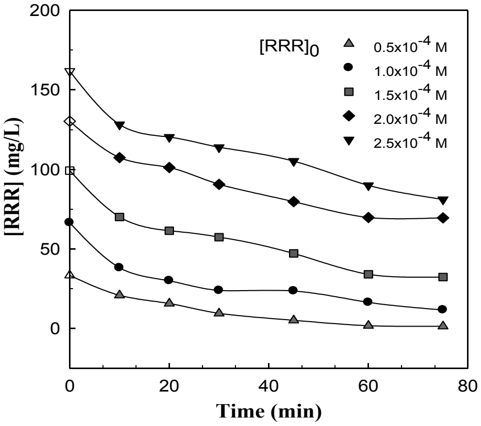

Fig.3. Variation of dye adsorption onto chitosan with time at different initial concentrations.

Effect of Temperature

The effect of temperature on adsorption kinetics of RRR onto chitosan was carried out at three different temperatures (30 ^{0}C, 40 ^{0}C and 50 ^{0}C) and constant pH 5.4 and at initial dye concentration of 1.0 × 10^{-4} M (Fig. 4). The results on dye adsorption at higher temperature would increase the mobility of the large dye ion and also produce a swelling effect within the internal structure of the chitosan, thus enabling the large dye molecule to penetrate further (Panday et al. 1989; Panday et al. 1968; Hiroyuki et al. 1994). The temperature affects the adsorption rate by altering the molecular interactions and the solubility (Panday et al. 1989). The higher removal due to increasing temperature may be attributed to chemical interactions taking place between the functional groups of the adsorbent and the dye.

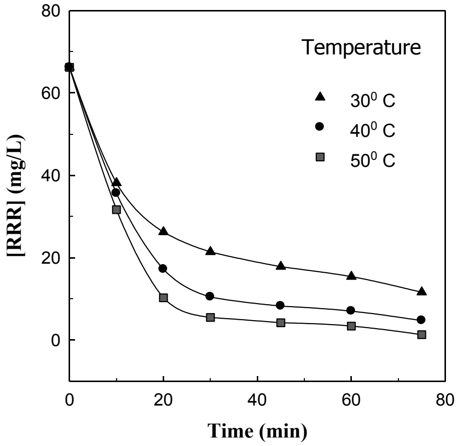

Fig. 4. Variation of dye uptake with time at different temperatures

Effect of pH

In order to avoid solubilization of the chitosan in aqueous solution at very low pH (Muzzarelli 1973), adsorption experiments were conducted with the pH ranging from 4.0 to 8.0. The effect of pH on adsorption kinetics of RRR onto chitosan at 30 ^{0}C is shown in Fig. 5 where the initial dye concentration was 1.0 × 10^{-4} M. It indicates that the adsorption rate (dq/dt) and the equilibrium adsorption capacity (q$_e$) is maximum at pH 5.4. It can be seen that the pH of aqueous solution plays an important role in the adsorption kinetics of RRR onto chitosan and the most suitable pH is 5.4 among the observed pH ranging from 4.0 to 8.0. The lower adsorption capacity of the dye on chitosan at lower pH may be related to the slight solubility at this pH. On the other hand, the lower adsorption capacity at higher pH should be expected from the lower positive charge on amino functional groups of chitosan which is less favourable for adsorption of anionic dye.

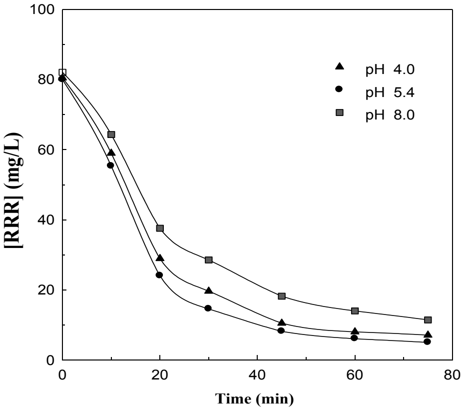

Fig. 5. Variation of dye uptake with time at different pHs.

Effect of particle size

Fig. 6. shows that as the particle size decreases, the adsorption of the dye increases and hence the removal of the dye increases. The equilibrium adsorption capacity (q$_e$) at particle sizes less than 200 nm (118.98 mg/g) is more than of that at particle sizes above 400 nm (90.09 mg/g). This is due to larger surface area that is associated with smaller particles. For larger particles, the diffusion resistance to mass transport is higher and most of the internal surface of the particle may not be utilized for adsorption and consequently, the amount of dye adsorbed is small (Mckay et al. 1983). It is also observed that as the particle size decreases, the dye uptake, that is the amount of dye adsorbed on the particles increases. Even though small particles are better for colour removal from the effluent, one cannot use small particles in a continuous packed bed adsorbed because of the high-pressure drops encountered. Such an effect is probably due to inability of the large dye molecule to penetrate all the internal pore structure of the chitosan and similar phenomenon was reported previously (Mckay 1964) for the adsorption of certain dyes on various adsorbents.

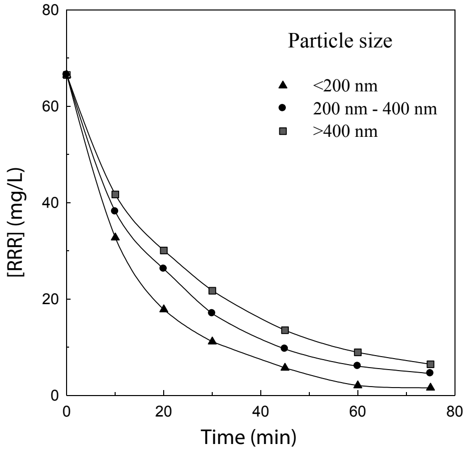

Fig. 6. Variation of specific dye adsorption with time at different particle sizes.

Kinetics of adsorption

In order to investigate the mechanism of adsorption kinetics the pseudo first-order and pseudo second-order equations were used to test the experimental data of initial concentration, temperature, pH and particle size respectively.

The pseudo first-order rate expression of Lagergren (Lagergren 1898) is given as:

$$\ln(q_e - q_t) = \ln q_e - k_1 t \text{ ……………..(1)}$$

Where, q_e and q_t are the amounts of dye adsorbed (mg/g) on chitosan at equilibrium and at time t, respectively, and k_1 is the rate constant of pseudo first-order adsorption (min^{-1}). Straight lines of $\ln(q_e - q_t)$ versus t suggests the applicability of this kinetic model to fit the experimental data. The slopes and intercepts of the plots were used to determine the k_1 and equilibrium adsorption capacity (q_e), which are shown in Fig. 7.

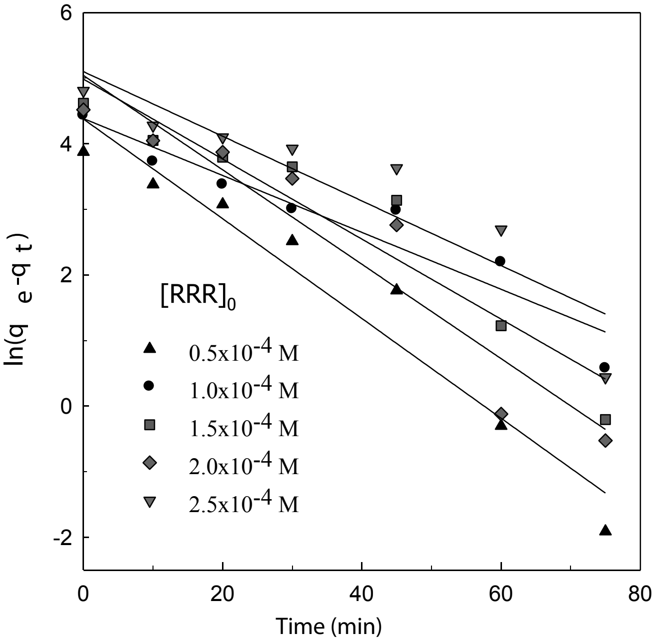

Fig. 7. Applicability of pseudo first order rate equation

The pseudo second-order kinetic model (McKay and Ho 1999) is expressed as:

$$t/q_t = 1/(q_e^2 k_2) + t/q_e \text{ ………………..(2)}$$

Where, k_2 (g/mg per min) is the rate constant of pseudo second-order adsorption. The values of k_2 were determined from the slopes of plots of t/q_t versus t. which is shown in Fig. 8.

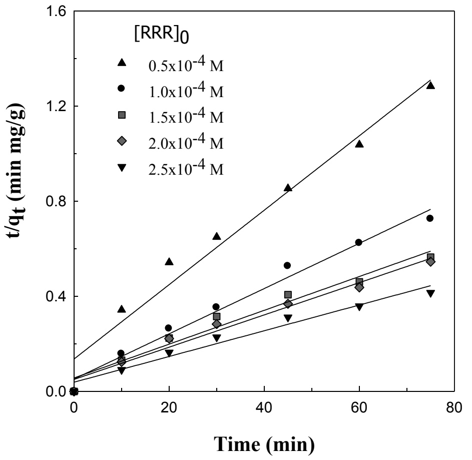

Fig. 8. Applicability of pseudo second order rate equation

From the comparison results of chitosan with the correlation coefficients (R^2) it is clear that the values of R^2 for the pseudo first order kinetics model were lower than pseudo second order model. Also, the calculated q_e values obtained from the pseudo first-order kinetic model do not give reasonable values, which are too low compared with experimental q_e values. These results suggest that the adsorption of dye RRR onto chitosan is not a pseudo first-order reaction. The slopes and intercepts of plots of t/q_t versus t were used to calculate the pseudo second-order rate constant k_2 and q_e. The straight lines in plot of t/q_t versus t show a good agreement of experimental data with the pseudo second-order kinetic model for different initial dye concentrations. The similar straight-line agreements are also observed for data at different temperatures, pHs and particle sizes (Figs are not shown). The rate constant k_2 at different temperatures was used to estimate the activation energy of the RRR adsorption onto chitosan.

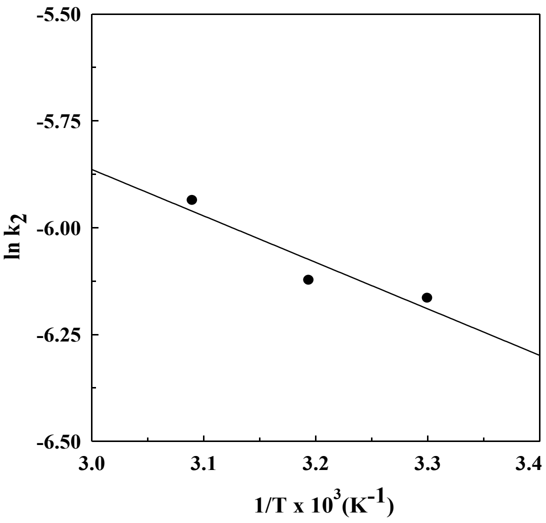

Fig. 9. A linear plot of lnk2 versus 1/T (K-1) to the adsorption of RRR on chitosan.

Table I. Comparison of pseudo first and pseudo second order rate constants, and calculated and experimental qe values of chitosan for different initial dye concentrations, temperatures, pHs and particle sizes

Parameters	Experimental	Pseudo-first order kinetics model			Pseudo- second order kinetics model		
	$q_{e(exp)}$ (mg/g)	k_1 (per min.)	$q_{e(cal)}$ (mg/g)	R^2	k_2 (g/mg per min.)	$q_{e(cal)}$ (mg/g)	R^2
pH							
4.0	110.24	0.0742	141.13	0.9889	0.00174	115.66	0.9940
5.4	113.35	0.0733	128.86	0.9855	0.00227	117.38	0.9909
8.0	103.72	0.0562	123.21	0.9723	0.00119	110.28	0.9854
Concentrations(M)							
0.5×10^{-4}	58.60	0.0761	79.85	0.9431	0.00180	63.90	0.9697
1.0×10^{-4}	105.28	0.0434	80.34	0.9067	0.00175	105.09	0.9822
1.5×10^{-4}	133.72	0.0610	146.70	0.9072	0.00090	140.65	0.9655
2.0×10^{-4}	138.10	0.0720	155.09	0.9043	0.00092	147.40	0.9738
2.5×10^{-4}	182.18	0.0493	164.40	0.8382	0.00076	184.76	0.9680
Temperature (°C)							
30	103.50	0.0428	63.52	0.9641	0.00210	106.18	0.9916
40	113.80	0.0560	70.75	0.9477	0.00219	118.13	0.9932
50	118.91	0.0584	64.96	0.8983	0.00264	122.63	0.9947
Particle size (nm)							
< 200	118.54	0.0757	111.72	0.9612	0.00177	124.55	0.9920
200 - 400	114.10	0.0601	100.06	0.9812	0.00132	121.36	0.9953
> 400	111.20	0.0516	95.27	0.9704	0.00114	118.80	0.9890

Assume that the correlation among the rate constant (k_2), temperature (T) and activation energy (Ea) follows the Arrhenius equation, which induces the following expression:

$$\ln k_2 = - E_a/R\ (1/T) + \text{const}\ldots\ldots\ldots\ldots\ldots(3)$$

Where, R is the molar gas constant. The slope of plot of $\ln k_2$ versus 1/T was used to evaluate E_a (Fig. 9). The value of E_a was estimated to be 9.25 kJ/mol. This value seems to be small and the adsorption rate is not very sensitive to the temperature in the range between 30°C and 50°C.

Adsorption isotherms of RRR onto chitosan

The adsorption isotherm indicates how the adsorbate molecules distribute between the liquid phase and the solid phase when the adsorption process reaches an equilibrium state. The analysis of equilibrium adsorption data by fitting them to different isotherm models is an important step to find the suitable model that can be used for design purposes (Haghseresht and Lu 1998). The adsorption isotherm study is applied on two well-known isotherms, the Langmuir and the Freundlich adsorption isotherm models. The applicability of the isotherm equation is compared by judging the correlation coefficients (R^2).

The well-known logarithmic form of the Freundlich isotherm (Freundlich 1906) is given by the following equation:

$$q_e = K_F C_e^{1/n}\ldots\ldots\ldots\ldots\ldots\ldots\ldots\ldots\ldots\ldots\ldots(4)$$

Equation (4) can be linearized by taking logarithms to find out the parameters K_F and 1/n

$$\ln q_e = \ln K_F + (1/n) \ln C_e\ \ldots\ldots\ldots\ldots.(5)$$

where q_e is the amount adsorbed at equilibrium (mg/g), C_e the equilibrium concentration of the adsorbate (RRR) and K_F and n are the Freundlich constants, n giving an indication of how favorable the adsorption process and K_F (mg/g.(L/mg)^n) is the adsorption capacity of the adsorbent. K_F can be defined as the adsorption or a distribution coefficient and represents the quantity of dye adsorbed onto chitosan adsorbent for a unit equilibrium concentration. The slope 1/n ranging between 0 and 1 is a measure of adsorption intensity or surface heterogeneity, becoming more heterogeneous as its value gets closer to zero. A value for 1/n below one indicates a normal Langmuir isotherm while 1/n above one is indicative of cooperative adsorption (Fytianos et al 2000).

The widely used Langmuir isotherm (Langmuir 1918) has found successful application in many real sorption processes and is expressed as:

$$q_e = K_L C_e/(1 + a_L C_e)\ldots\ldots\ldots\ldots\ldots\ldots\ldots\ldots(6)$$

The constants K_L and a_L are the characteristics of the Langmuir equation and can be determined from a linearized form of this equation, represented by Equation (7):

$$C_e/q_e = 1/K_L + (a_L/K_L)C_e \ldots\ldots\ldots\ldots\ldots\ldots (7)$$

Where, C_e is the equilibrium concentration of the adsorbate (RRR) (mg/L), q_e, the amount of adsorbate adsorbed per unit mass of adsorbate (mg/g), K_L and a_L are the equilibrium constant and affinity of adsorbent towards adsorbate, respectively and the ratio a_L/K_L gives the inverse of theoretical monolayer saturation capacity (q_m). When C_e/q_e was plotted against C_e, a straight line with slope of (a_L/K_L) was obtained, indicating that the adsorption of the RRR on chitosan follows the Langmuir isotherm. The Langmuir constants a_L, K_L and q_m were calculated from this isotherm and their values are given in Table II. As seen from Table II, the Langmuir model yields a somewhat better fit ($R^2 \geq 0.98$) than the Freundlich model ($R^2 \geq 0.89$).

The essential characteristics of the Langmuir isotherm can be expressed in terms of a dimensionless equilibrium parameter (R_L) (Hall et al. 1966), which is defined by:

$$R_L = 1/\ (1 + a_L C_h) \ldots\ldots\ldots\ldots\ldots\ldots\ldots (8)$$

Where, a_L is the Langmuir constant and C_h is the highest dye concentration (mg/L). The value of R_L indicates the type of the isotherm to be either unfavorable ($R_L > 1$), linear ($R_L = 1$), favorable ($0 < R_L < 1$) or irreversible ($R_L = 0$) (Table II). The value of R_L was varied from 0.022 to 0.046 for all of the parameters and confirmed that the chitosan is favorable for adsorption of the RRR dye under conditions used in this study.

The thermodynamic parameters such as change in free energy (ΔG), enthalpy (ΔH) and entropy (ΔS) were determined using following equations (Chiou and Li 2003):

$$\Delta G = -RT\ln K_L \ldots\ldots\ldots\ldots\ldots\ldots\ldots\ldots (9)$$

$$\ln K_L = \Delta S/R - \Delta H/RT \ldots\ldots\ldots\ldots\ldots (10)$$

Where, K_L is the equilibrium constant, T is the solution temperature (K) and R is the molar gas constant. ΔH and ΔS were calculated from the slope and intercept of van't Hoff plots of $\ln K_L$ vs. 1/T (Fig. 10). The results are presented in Table III. The negative values of ΔG and positive value of ΔH indicate that the adsorption of RRR on chitosan is spontaneous and an endothermic process. These behaviors seem to be explained by the chemical interactions in the dye RRR-chitosan system. The positive value of ΔS suggests that

Table II. Freunlich and Langmuir isotherm constants at different pHs, temperatures and particle sizes

Parameters	Freundlich			Langmuir				
pH	K_F (mg/g. (L/mg)^n) n	n (g/L)	R^2	K_L (L/g)	a_L (L/mg)	q_m (mg/g)R_L	K_L	R^2
4.0	50.8082	3.0891	0.8937	34.4236	0.1745	197.29	0.0277	0.9997
5.4	59.4389	3.0562	0.9246	47.6385	0.2179	218.58	0.0223	0.9992
8.0	40.8289	2.9755	0.9233	24.0894	0.1362	176.87	0.0352	0.9982
Temperature (^{0}C)								
30	46.3444	4.4763	0.9957	14.5773	0.1020	142.86	0.0464	0.9855
40	52.8205	4.7059	0.9924	18.4162	0.1215	151.52	0.0392	0.9816
50	45.3541	3.7161	0.9678	18.3486	0.1138	161.29	0.0418	0.9861
Particle size (nm)								
< 200	73.2544	4.2028	0.9962	41.2391	0.1956	210.88	0.0247	0.9967
200 - 400	60.2195	4.4491	0.9887	26.3504	0.1513	174.12	0.0318	0.9878
> 400	56.4038	5.1471	0.9803	22.1890	0.1528	145.23	0.0315	0.9845

entropy is responsible for making the ΔG negative for the adsorption process to be spontaneous.

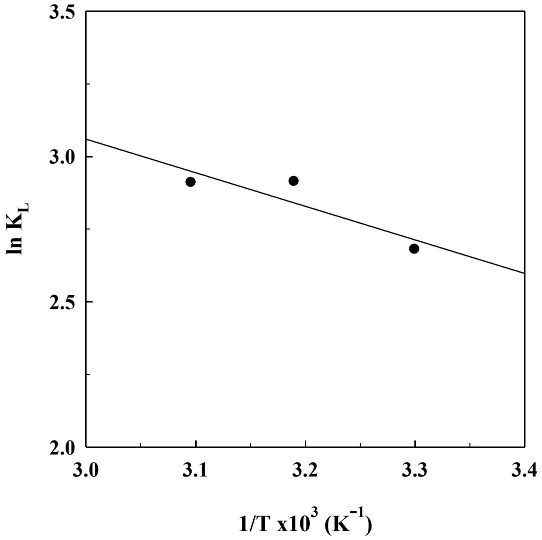

Fig. 10. A linear plot of lnKL versus 1/T (K-1) to the adsorption of RRR on chitosan

Table III. Thermodynamic parameters for the adsorption of dye RRR onto Chitosan

Temperature (K)	ΔG (kJ/mol)	ΔH (kJ/mol)	ΔS (JK^{-1}/mol)	R^2
303	-6.75			
9.46	53.82	0.7541	313	-7.34
323	-7.33			

Conclusion

Batch experiments showed that the equilibrium adsorption capacity (q_e) of chitosan increases with increasing the initial concentration of dye, temperature and with decreasing particle size. However, the highest adsorption capacity has been found at a pH about 5.4. The strong electrostatic interaction between the $–NH_3^+$ of chitosan and dye anions can be used to explain the high adsorption capacity of anionic dyes onto chitosan. The pseudo second-order kinetic model and Langmuir adsorption isotherm agree very well with the adsorption of dye RRR on chitosan. It may be concluded that chitosan is a suitable adsorbent for adsorption of RRR. Adsorption of hundred percentage is possible under optimum conditions of temperature, adsorbent dosages, particle size range and pH. The use of chelating polymer (chitosan) for adsorption process was technically and economically feasible. The dye adsorbed on chitosan can be easily regenerated and could be further used in the application of membranes and biochemical areas. Therefore, chitosan used as medium for removing the reactive dye from wastewater can be a feasible and potential alternative for the decolorization of wastewater.

References

Aksu Z (2001), Biosorption of Reactive Dyes by Dried Activated Sludge: Equilibrium and Kinetic Modeling, *Bio-chemical Engineering Journal*, **7**: 79-84.

Arami M, Limaee N Y, Mahmoodi N M and Tabrizi N S (2006), Equilibrium and Kinetics Studies for the Adsorption of Direct and Acid Dyes from Aqueous Solution by Soy Meal Hull, *Journal of Hazardous Materials* **135**: 171-179.

Chiou M S and Li H Y (2002), Equilibrium and Kinetic Modeling of Adsorption of Reactive Dye on Cross-Linked Chitosan Beads, *Journal of Hazardous Materials,* **93**: 233-248.

Chiou M S and Li H Y (2003), Adsorption Behavior of Reactive Dye in Aqueous Solution on Chemical Cross-Linked Chitosan Beads, *Chemosphere,* **50**: 1095-1105.

Chowdhury A K Sarkar A D and Bandyopadhyay A (2009), Rice husk ash as a low cost adsorbent for the removal of methylene blue and congo red in aqueous phases, *Clean,* **37**: 581-591.

Chu K H (2002), Removal of Copper from Aqueous Solution by Chitosan in Prawn Shell: Adsorption Equilibrium and Kinetics, *Journal of Hazardous Materials*, **90**: 77-95.

Fernandes A N, Almeida C A P, Menezes C T B, Debacher N A and Sierra M M D (2007), Removal of Methylene Blue from Aqueous Solution by Peat, *Journal of Hazardous Materials,* **144**: 412-419.

Freundlich H (1906), Adsorption Solution, *Zeitschrift für Physikalische Chemie*, **57**: 384-470.

Fytianos K, Voudrias E and Kokkalis E (2000), Sorption–desorption behavior of 2, 4-dichlorophenol by marine sediments, *Chemosphere,* **40**: 3–6.

Haghseresht F and Lu G (1998), Adsorption characteristics of phenolic compounds onto coal-reject-derived adsorbents, *Energy Fuels,* **12**: 1100–1107.

Hall K R, Eagleton L C, Acrivos A and Vermeulen T (1966), Pore and solid diffusion kinetics in fixed bed adsorption under constant pattern conditions, *Industrial and Engineering Chemistry Fundamentals,* **5**: 212–223.

Hiroyuki H, Fukuda S, Okamoto A and Kataoka T (1994), Adsorption of acid dye cross-linked chitosan fibers-Equilibria, *Chem. Egg. Sci,* **48**: 2267- 2272.

Lagergren S (1898), Zur Theorie der Sogenannten Adsorption Geloster Stoffe, *K Sven Vetenskapsakad Handl,* **24**: 1-39.

Langmuir I (1918), Adsorption of Gases on Plain Surfaces of Glass Mica Platinum, *Journal of American Chemical Society,* **40**: 1361-1403.

Lazaridis N K, Kyzas G Z, Vassiliou A A and Bikiaris D N (2007), Chitosan Derivatives as Biosorbents for Basic Dyes, *Langmuir,* **23**: 7634-7643.

McKay G, Blair H S and Gardner J R (1982), Adsorption of Dyes on Chitin, *J. Appl Polym. Sci,* **27**: 3043-3057.

Mckay G, Blair H S and Gardner J R (1983), Rate studies for adsorption of dyestuff on chitin, *J Coll. &Interface Sci,* **95**: 108-119..

Mckay G (1964), Adsorption of acid dye and basic dyes into activated carbon in fluidized beds, *Chem. Eng. Res. Des,* **6**: 29-35.

McKay G and Ho Y S (1999), Pseudo-Second Order Model for Sorption Processes, *Process Biochemistry,* **34**: 451-465.

Modak P R, Singh K S and Connor D A (2009), Experimental Study on the Elimination of Colour and Organic Matter from Wastewater using an Inexpensive Biomaterial, Chitosan, *Water Quality Research Journal of Canada,* **44**: 295-306.

Muzzarelli R A A (1973), Natural Chelating Polymers: Alginic Acid, Chitin and Chitosan, *Pergamon*, Oxford.

Panday K K, Prasad Cl and Singh VN (1989), Use of wollastonite for the treatment of Cu (II) rich effluents, *Water Res,* **19**: 869-872.

Panday K K, Prasad G and Singh V N (1968) Copper removal from aqueous solution by fly ash, *Water Air and Soil Poll,* **27**: 287-292..

Racyte J, Rimeika M and Bruning H (1999) pH Effect on Decolorization of Raw Textile Wastewater Polluted with Reactive Dyes by Advanced Oxidation with UV/H_2O_2, *Environmental Protection Engineering,* **35**: 167-178.

Raïs Z, El Hassani L, Maghnouje J, Hadji M, Ib-nelkhayat R, Nejjar R, Kherbeche A and Chaqroune A (2002) Removal from Textile Wastewater by Phosphogypsum using Coagulation and Precipitation Method, *Physicsand Chemistry News,* **7**: 100-109.

Rangel-Mendez J R, Monroy-Zepeda R, Leyva-Ramos ., Diaz-Flores P E and Shirai K (2009), Chitosan Selectivity for Removing Cadmium(II), Copper(II), and Lead(II) from Aqueous Phase: pH and Organic Matter Effect, *Journal of Hazardous Materials,* **162**: 503-511.

Rezaee A, Ghaneian M T, Hashemian S J, Mous-savi G, Khavanin A and Ghanizadeh G (2008), Decolorization of Reactive Blue 19 Dye from Textile Wastewater by the UV/H2O2 Process, *Journal of Applied Sciences,* **8**: 1108-1112.

Rodriguez A, Garcia J, Ovejero G and Mestanza M (2009), Adsorption of Anionic and Cationic Dyes on Activated Carbon from Aqueous Solutions: Equilibrium and Kinetics, *Journal of Hazardous Materials,* **172**: 1311-1320.

Saha T K, Ichikawa H and Fukumori Y (2006), Gadolinium Diethylenetriaminopetaacetic Acid-Loaded Chitosan Microspheres for Gadolinium Neutron-Capture Therapy, *Carbohydrate Research,* **341**: 2835-2841.

Saraswathi R and Saseetharan M K (2010), Investigation on Microorganisms and their Degradation Efficiency in Paper and Pulp Mill Effluent, *Journal of Water Resource and Protection,* **2**: 660-664.

Tsuboy M S, Angeli J P F, Mantovani M S, Knasmueller S, Umbuzeiro G A and Ribeiro L R (2007), Genotoxic, Mutagenic and Cytotoxic Effects of the Commercial Dye CI Disperse Blue 291 in the Human Hepatic Cell Line HepG2, *Toxicology in Vitro*, **21**: 1650-1655.

Varlikli C, Bekiari V, Kus M, Boduroglu N, Oner I, Lianos P, Lyberatos G. and Icli S (2009), Adsorption of Dyes on Sahara Desert Sand, *Journal of Hazardous Materials,* **170**: 27-34.

Vinitnantharat S, Chartthe W and Pinisakul, A (2008), Toxicity of Reactive Red 141 and Basic Red 14 to Algae and Waterfleas, *Water Science and Technology,* **58**: 1193-1198.

Received: 7 October 2013; Revised: 25 February 2014; Accepted: 28 May 2014.